Published in final edited form as:
Nat Methods. 2007 September ; 4(9): 733–739. doi:10.1038/nmeth1077.

An HSV vector system for selection of ligand-gated ion channel modulators

Rahul Srinivasan[1], **Shaohua Huang**[1], **Suchita Chaudhry**[1], **Adrian Sculptoreanu**[2], **David Krisky**[3], **Michael Cascio**[1], **Peter A Friedman**[2], **William C de Groat**[2], **Darren Wolfe**[1], and **Joseph C Glorioso**[1]

[1]Department of Molecular Genetics and Biochemistry, 200 Lothrop Street, Biomedical Science Tower, University of Pittsburgh, Pittsburgh, Pennsylvania 15261, USA

[2]Department of Pharmacology, 200 Lothrop Street, Biomedical Science Tower, University of Pittsburgh, Pittsburgh, Pennsylvania 15261, USA

[3]Department of Pathology, 200 Lothrop Street, Biomedical Science Tower, University of Pittsburgh, Pittsburgh, Pennsylvania 15261, USA

Abstract

Pathological alterations of ion channel activity result from changes in modulatory mechanisms governing receptor biology. Here we describe a conditional herpes simplex virus (HSV) replication–based strategy to discover channel modulators whereby inhibition of agonist-induced channel activation by a vector-expressed modulatory gene product prevents ion flux, osmotic shock and cell death. Inhibition of channel activity, in this case, the rat vanilloid (Trpv1) or the glycine receptor (GlyRα1), can allow selection of escape vector plaques containing the 'captured' modulatory gene for subsequent identification and functional analysis. We validated this prediction using mixed infections of a wild-type Trpv1 expression vector vTTHR and a nonfunctional 'poreless' Trpv1 subunit–expressing vector, vHP, wherein vHP was highly selected from a large background of vTTHR viruses in the presence of the Trpv1 agonist, capsaicin. The approach should be useful for probing large libraries of vector-expressed cDNAs for the presence of ion channel modulators.

The human genome encodes over 400 ion channels involved in various biological functions[1]. Channel inhibitors such as the anesthetic lidocaine[2], the anticonvulsant agent levetiracetam[3], the antiarrhythmic agent carvedilol[4], the anticancer agent carboxyamidotriazole[5] and the antiemetic agent ondansetron[6] provide valuable treatment options, but cause serious adverse reactions because of a widespread distribution of the targeted receptor. Insights into ion channel modulation can reveal new targets for regulating channel activity with greater specificity. For example, allostery is an extensively studied phenomenon in which modulatory agents enhance or depress channel function by action on allosteric sites distant from the orthosteric agonist-binding site[7]. Modulatory mechanisms of

Correspondence should be addressed to J.C.G. (glorioso@pitt.edu).

Note: Supplementary information is available on the Nature Methods website.

AUTHOR CONTRIBUTIONS: R.S. and J.C.G. wrote the manuscript. R.S. engineered the vTTHR and vHP vectors and either performed or was directly involved in all the experiments. S.H. and D.K. engineered vHG and vTT viral vectors. S.C. performed experiments for poreless Trpv1. A.S. performed electrophysiological recordings. M.C. provided the *GLRA1* cDNA and advised R.S. on glycine selection experiments. P.A.F. performed calcium influx studies. W.C.D. advised R.S. and A.S.; J.C.G. and D.W. advised R.S.

COMPETING INTERESTS STATEMENT: The authors declare no competing financial interests.

ion channels have been uncovered by fluorescence-based assays including fluorescent resonance energy transfer to study receptor assembly and fluorescence recovery after photobleaching to assess cell-surface movement of the receptor, whereas ion channel pharmacology is evaluated by fluorescence imaging (FLIPR) and electrophysiology[8,9]. Other important strategies use yeast-based microbial selection to identify mutations affecting channel function[10]. Methods to identify gene products influencing mammalian ion channel function, however, have not been described yet.

HSV vectors offer a new approach to identify genes that have a role in ion channel regulation. Advantages of HSV vectors include high-efficiency transduction of most cell types, the efficient expression of biologically active ion channels *in vitro* or *in vivo*, as well as the capability to accommodate multiple transgenes. Additionally, methods to construct cDNA and siRNA vector libraries and the screening techniques to identify gene products involved in ion channel modulation are in development. HSV vectors should therefore provide powerful strategies to dissect signaling pathways controlling ion channel function (activation, sensitization, desensitization) and methods to identify modulators of channel assembly, trafficking and turnover.

In this study we exploited these properties of HSV vectors to develop and characterize a virus-based assay that can be used to identify ligand-gated ion channel modulators. Our experiments showed that activation of two different HSV vector-expressed ligand-gated ion channels, the rat vanilloid receptor 1 (Trpv1) and alpha-1 homopentamers of the human glycine receptor (GlyRα1) resulted in impaired virus replication. The disruption of channel activity by chemical antagonists or a vector-expressed Trpv1 modulatory gene product, poreless Trpv1, sustained active virus production. In these latter studies, escape viruses expressed poreless Trpv1, indicating that the HSV-based selection method should be useful for capturing and identifying new ion channel modulators from vector-expressed cDNA libraries.

Results

HSV vector-mediated expression of Trpv1

We constructed a replication-defective backbone HSV-1 vector deleted for the essential immediate early genes, *ICP27* and *ICP4*. These vectors lack early and late gene expression, and are propagated in complementing cells (7b) supplying the missing gene products in *trans*[11]. The test vector, vTT is derived from this replication-defective backbone and contains *Trpv1* cDNA driven by the early thymidine kinase (*tk*) promoter (Fig. 1a). *Trpv1* replaces both immediate early *ICP4* genes and is exclusively expressed in complementing 7b cells (20 h post-infection (h.p.i.); multiplicity of infection (MOI) = 1; Fig. 1) because in these cells the virus can replicate and activate promoters with early and late kinetics. The rationale for using this replication-defective construct is to express Trpv1 as an early gene product so that modulatory gene expression occurs as an immediate early gene in advance of Trpv1 expression and will hence have the greatest opportunity for inhibiting Trpv1 activity. The control vector, vHG had the same mutant background as vTT, except that we replaced the *ICP4* genes with an enhanced green fluorescent protein (*EGFP*) transgene under control of the human cytomegalovirus (HCMV) immediate early gene promoter (Fig. 1a). As EGFP expression is driven by an immediate early promoter, it is expressed in complementing 7b cells as well as in noncomplementing Vero cells (Fig. 1b).

HSV-expressed Trpv1 is functional

We demonstrated vTT-expressed Trpv1 functionality in 7b cells by whole-cell patch clamp recordings. Control vHG-infected 7b cells did not respond to capsaicin (Fig. 2a), whereas

capsaicin stimulation (0.5 μM) of vTT-infected 7b cells at 20 h.p.i. and a MOI of 5 resulted in large (6 ± 3 nA; ± s.e.m., $n = 7$), slowly desensitizing, biphasic inward currents (time constant (τ) = 280.6 ± 45 s; ± s.e.m., $n = 7$; Fig. 2b). Addition of 5 μM of the Trpv1 antagonists SB-366791 (ref. 12), ruthenium red and diaryl piperazine[13] (NDT9515223), completely blocked capsaicin currents (data not shown). These data demonstrated that vector-expressed Trpv1 activity was Trpv1-dependent and qualitatively similar to that of neuronal Trpv1 (refs. 14–16).

Trpv1 activation results in Ca^{2+} influx

We next monitored intracellular calcium levels after Trpv1 activation in vTT-infected 7b cells. Capsaicin-induced activation of the vector-expressed Trpv1 caused a concentration-dependent and sustained influx of Ca^{2+} ions in 7b cells after addition of 0.3 and 3.0 μM capsaicin (Supplementary Fig. 1a,c online). Application of ionomycin after capsaicin treatment enhanced maximal Ca^{2+} response resulting from addition of 0.3 μM capsaicin but had no effect on the response from 3.0 μM capsaicin, suggesting that 3.0 μM capsaicin induced maximal millimolar intracellular [Ca^{+2}]. As GFP would interfere with FURA-2 measurements, we used the vector QOZ as a negative control for intracellular Ca^{2+} measurements. QOZ has a backbone that is similar to that of vHG, but lacks the *HCMVp-EGFP* cassette at the *ICP4* locus. QOZ instead contains an *ICP0p-LacZ* cassette at the *UL41* locus. QOZ-infected cells did not respond to capsaicin (Supplementary Figs. 1b,d). These data demonstrate that vTT-expressed Trpv1 functioned as a calcium ion channel in 7b cells.

Trpv1 activation causes cell death

Mitochondrial permeability transition (MPT) precedes cell death and occurs in Vero cells after ion influx-induced hyperosmotic shock[17]. After stimulation with 3 μM capsaicin, we observed MPT in vTT-infected (Supplementary Fig. 2 online) but not in QOZ-infected 7b cells at 12 h.p.i. with an MOI of 0.3. (Supplementary Fig. 2d). The 7b cells with capsaicin-induced MPT were visibly swollen (Supplementary Fig. 2b). These data provide evidence for activated Trpv1 triggering intracellular ion overload, leading to MPT and hyperosmotic shock in 7b cells.

Trpv1 activation blocks vector replication

Because capsaicin caused Trpv1 activation, Ca^{2+} influx, MPT and cell death, we anticipated that vTT-expressed Trpv1 activation would block virus replication. To quantify the effects of Trpv1 activation on viral replication, we exposed vTT-infected 7b cells (MOI of 0.01) to a range of capsaicin concentrations (0.1–40 μM). We determined the differences between vHG (control) and vTT (Trpv1-expressing) vector growth as ratios of vHG to vTT virus particle yield (growth ratio) at each capsaicin concentration. We observed a growth ratio differential of about 500-fold at 72 h.p.i. with 3 μM capsaicin (Fig. 3a). To validate the system using multiple Trpv1 agonists, we repeated the above experimental procedure with resiniferatoxin, an ultrapotent Trpv1 agonist. Nanomolar concentrations of resiniferatoxin caused a similar reduction in vTT viral titers (Fig. 3b). These data validate the use of Trpv1 agonists to conditionally inhibit HSV vector replication.

Trpv1 antagonism rescues vector replication

To show that antagonism of capsaicin-induced Trpv1 receptor activation should rescue vector replication, we determined virus yields after infections with capsaicin or with both capsaicin and known Trpv1 antagonists. We added ruthenium red to replication assays along with capsaicin. Vector-infected 7b cells were plated with 3 μM capsaicin, 5 μM ruthenium red, or 3 μM capsaicin + 5 μM ruthenium red. Addition of 3 μM capsaicin specifically inhibited vTT replication at 24, 48 and 72 h.p.i. In the presence of both 3 μM capsaicin and

5 μM ruthenium red, replication of vTT was completely restored (Fig. 4a). We carried out similar assays using another known Trpv1 antagonist, SB-366791 (ref. 12). vTT replication was not affected by the addition of 1 and 10 μM SB-366791 alone (data not shown). We observed dose-dependent rescue of vTT viral titers in the presence of 1 and 10 μM SB-366791 with 0.5 μM capsaicin (Fig. 4b). None of the chemicals used affected replication of the control vector, vHG.

Application of HSV vectors to GlyRα1 receptors

To generalize our HSV-based selection system to other ligand-gated ion channels, we carried out similar experiments using a vector that expressed the anion channel, GlyRα1. GlyRα1 belongs to the nicotinoid subfamily of ion channels and has a pharmacological profile that is distinct from Trpv1. A cDNA encoding the human alpha-1 glycine receptor subunit (*GLRA1*) was recombined into the *ICP4* locus of vHG to create the vector, vHGlyRα1, which was identical to vTT (Fig. 1a), except that the *GLRA1* cDNA was under control of the HCMV immediate early gene promoter. Immunostaining for the gene product, GlyRα1 in vHGlyRα1-infected Vero and 7b cells (20 h.p.i. and MOI of 1) confirmed immediate early promoter–induced vector expression of GlyRα1 (Supplementary Fig. 3a,d online).

Whole-cell patch clamp recordings of vHGlyRα1-infected 7b cells demonstrated concentration-dependent inward currents after application of 5 or 50 μM glycine, consistent with glycine-induced Cl^- efflux from vHGlyRα1-infected cells (Supplementary Fig. 4a–c online). GlyRα1 desensitized rapidly at elevated glycine concentrations, similar to the behavior of native glycine receptor (GlyR)[18,19] (Supplementary Fig. 4d). All currents were completely inhibited by 5 μM of strychnine, a GlyR-specific antagonist (Supplementary Fig. 4a,b).

vHGlyRα1 vector replication with glycine and strychnine

After confirmation of HSV-expressed GlyRα1 functionality, we performed virus replication assays to assess the effects of the GlyRα1-specific agonist, glycine, and the antagonist, strychnine on vHGlyRα1 growth. We demonstrated that when compared with vHG growth, 200 μM glycine inhibited vHGlyRα1 replication and caused a growth ratio differential of about 3,800-fold (72 h.p.i. and MOI of 0.01; Supplementary Fig. 5 online). Growth inhibition was accompanied by a visible shrinkage of vHGlyRα1-infected cells, consistent with hypo-osmotic shock and cell death as a result of glycine-induced Cl^- efflux. We found that 400 and 800 μM glycine also inhibited vHGlyRα1 replication to a similar extent (data not shown). vHGlyRα1 replication was completely restored by coincubation with 5 μM strychnine (Supplementary Fig. 5). These experiments demonstrate that the HSV-based selection described here can be used as a platform assay for ligand-gated ion channel modulation.

Selection for a gene-encoded modulator of Trpv1

To validate the selection system for identifying new ligand-gated ion channel modulators, we used a model negative modulator of Trpv1 activity deleted for the channel pore–forming domain. This channel, designated poreless Trpv1, has been previously shown to coassemble with wild-type Trpv1 subunits to form capsaicin-insensitive, Ca^{2+}-impermeable channels[20]. Thus we predicted that coinfection of vectors that express wild-type Trpv1 (vTT) and poreless Trpv1 (vHP) would result in the selection of porelessTrpv1 vector plaques in the presence of capsaicin. Both the mutant Trpv1 product poreless and wild-type Trpv1 were expressed in a similar fashion in complementing cells (Fig. 5). To facilitate a visual distinction of vHP from vTT plaques, we introduced the red fluorescent protein (RFP) *DsRed2* gene into the vTT backbone (Fig. 5a). The resulting virus, vTTHR was capsaicin-

sensitive (Fig. 5c) and produced red plaques (Fig. 5a), whereas vHP was resistant to capsaicin exposure (Fig. 5c) and produced clear plaques. vTTHR titers were reduced from 10^7 p.f.u./ml to about 2,000 p.f.u./ml, whereas vHP titers were unaffected by capsaicin.

Southern blot analysis with a *Trpv1* cDNA probe (*Asp*718-*Not*I fragment) indicated the absence of *Trpv1* cDNA in the vHG genome (Fig. 5b). vTTHR lanes contained a 3-kb band corresponding to *Trpv1* cDNA fragment with both *Ban*HI as well as *Bam*HI and *NdeI* restriction digests, whereas vHP displayed a single 3-kb band when digested with *Bam*HI. vHP DNA digested with *Bam*HI and *NdeI* displays 2-kb and 1-kb bands, indicating the insertion of a diagnostic *NdeI* site into *Trpv1* to create poreless *Trvp1*.

Using coinfection experiments we showed that indeed vHP was readily selected in a background of vTTHR particles, which could be enriched by a second round of capsaicin-dependent selection. For vHP selection experiments, 250,000 7b cells were co-infected with vHP (MOI of either 0.03 or 0.003) and vTTHR (MOI of 3), expressed as 0.99% or 0.099% vHP input. In both instances, a single round of capsaicin exposure for 72 h.p.i. resulted in selection of clear vHP plaques (about 17 and 5%, respectively for each MOI; Fig. 6). We titered the supernatants from the first round of selection and used them to coinfect 7b cells at an MOI of 3. We then plated vector-infected 7b cells as infectious centers in 96-well plates and subjected them to a second round of selection with capsaicin for 72 h.p.i. In a second round of selection with capsaicin, vHP output percentages were greatly enriched (about 83 and 40%, respectively for each MOI; Fig. 6). Randomly picked clear plaques after each round of selection confirmed the presence of the poreless gene by diagnostic Southern blot (Fig. 5b). As an experimental control, we modeled the frequency at which escape viral plaques not expressing a relevant modulatory gene product occur. To do this, we performed similar experiments in which vHP was replaced with vHG (Fig. 1a), allowing the detection of vHG as green plaques in a background of red plaques. The frequency of green plaques was 2.71% with a vHG input of 0.99% and 0% with a vHG input of 0.099% (Fig. 6).

Discussion

Here we describe a method to discover modulators of ion channel activity based on the selective replication of HSV vectors that coexpress an ion channel and a modulatory gene product. In the absence of the modulatory product, agonist-induced ion channel activation results in osmotic shock and the loss of virus replication. The presence of a vector-expressed modulatory gene product will interfere with ion channel function, and virus replication allows the ‘capture’ of the modulator gene as part of the actively replicating virus genome. Because these vectors cannot replicate in noncomplementing cells such as neurons, the modulatory gene products can ultimately be directly studied for their effects on endogenously expressed ion channels after vector-mediated gene delivery.

The high levels of intracellular [Ca^{+2}] observed after 3.0 μM capsaicin-induced Trpv1 activation caused calcium overload and MPT. This resulted in visible cell swelling, consistent with hyper-osmotic shock and Vero cell death[17]. A source of potential false positives in our HSV based assay—when used for Ca^{2+} channels—can be the identification of candidate vectors encoding rapid Ca^{+2} buffering proteins and MPT or apoptosis inhibitors, as these vectors may allow replication in the presence of agonists. These gene products are of great interest as a therapeutic approach to treat neuronal apoptosis resulting from spinal cord injury or degenerative disorders[21].

The Trpv1 agonists, capsaicin and resiniferatoxin caused a large dose-dependent reduction in vTT replication compared to control vHG vector, indicative of a specific effect of the agonists on the Trpv1 receptor. Resiniferatoxin was effective in reducing vTT viral titers at

nanomolar concentrations compared to micromolar concentrations of capsaicin. This dosage phenomenon agrees with the fact that resiniferatoxin is a several-fold more potent Trpv1 agonist than capsaicin. The known Trpv1 antagonists, ruthenium red and SB-366791 rescued vTT replication, thus validating our selection rationale based on virus growth recovery.

Studies using the GlyRα1 receptor demonstrated that HSV-based selection could be extended to this chloride ion channel. Notably, the results showed that glycine caused a dose-dependent reduction in virus yield that was reversible with strychnine, a known GlyRα1 antagonist. The large difference in growth ratios observed for the two receptors (500-fold for Trpv1 versus 3,800-fold for GlyRα1) may be explained either by the different mechanisms of action of the two receptors or by differences in the timing and amount of receptor expression produced by the immediate early HCMV promoter versus the later acting *tk* promoter.

Ion channels are subject to complex regulation at transcriptional and post-translational levels[22]. The HSV replication–based method described here can be used to identify ion channel modulators at each of these levels. In this study we modeled the potential for selecting vectors expressing gene-encoded inhibitors of Trpv1 channel activity at the post-translational level by mixed infections of vTT and vHP, a vector that expresses a dominant-negative inhibitor of Trpv1 referred to as poreless Trpv1 (ref. 20). Poreless Trpv1 subunits coassemble with wild-type receptor subunits, creating a defective channel that is not responsive to capsaicin and will not allow calcium influx[20]. Coinfection of wild-type Trpv1 vector (vTTHR) with the poreless Trpv1 vector (vHP) at vHP inputs of either 0.99 or 0.099% demonstrated that vHP was readily detected with a minimum of potential false positives. This vHP output could be enriched with a second round of capsaicin selection, allowing sequential selection and enrichment strategies to be used. Experiments are in progress to test this method using additional model antagonist genes that inhibit ion channel function.

The method described here suggests that vectors expressing highly diverse cDNA or siRNA libraries can be used in HSV-based selection, where 1,000 library members can be screened in separate pools for genes that inhibit agonist-induced channel activation. Alternatively, the library could be designed to consist of antisense mRNAs to identify new genes that are essential for ion channel activation.

Methods

Cell culture and chemicals

We maintained cells in Dulbecco's Minimum Essential Medium (DMEM) supplemented with 10% fetal bovine serum (FBS; Invitrogen). All chemicals were obtained from Sigma. We performed experiments with vHGlyRα1 using glycine free minimum essential medium (MEM) supplemented with 10% glycine-depleted dialyzed FBS (Invitrogen).

HSV-1 vector constructs

To construct recombinant viruses, we recombined plasmids into targeted loci of the parent virus by sequential virus infection and plasmid transfection and then screened for recombinant vectors by marker transfer[23]. We purified potential recombinants by three rounds of limiting dilution, verified the genome by Southern blot analysis and then expanded, titered, aliquoted and stored confirmed virus stocks at −80 °C. We engineered the vectors as follows: the QOZHG virus (*ICP4*$^{-}$, *ICP27*$^{-}$, *ßICP22*, *ßICP47*, *ICP0p*$^{-}$*LacZ*::*UL41*, *HCMVp: EGFP*::*ICP27*)[24] was deleted for the EGFP expression cassette by homologous recombination with a plasmid containing flanks for the *UL54*

(*ICP27*) coding sequence to create vector, QOZ (*ICP4*$^{-}$, *ICP27*$^{-}$, *ßICP22*, *ßICP47*, *ICP0p-LacZ::UL41*). We then deleted the *ICP0p-LacZ* cassette from QOZ to create vector Q. We engineered an HCMV immediate early promoter driving EGFP into the *ICP4* loci of the Q vector to create vector vHG (*ICP4*$^{-}$, *ICP27*$^{-}$, *ßICP22*, *ßICP47 HCMVp-EGFP::ICP4*) that has an *ICP4* and *ICP27* deletion, truncated *ICP22* and *ICP47* promoters and contains two copies of the *HCMVp-EGFP* expression cassette at *ICP4* loci. The vTT (*ICP4*$^{-}$, *ICP27*$^{-}$, *ßICP22*, *ßICP47*, *TKp-Trpv1::ICP4*) and vHGlyRα1 *(ICP4*$^{-}$, *ICP27*$^{-}$, *ßICP22*, *ßICP47*, *HCMVp-GLRA1::ICP4*) vectors were constructed by replacing the *HCMVp-EGFP* cassette in the *ICP4* loci of vHG with either the rat *Trpv1* cDNA[25] or a human *GLRA1* cDNA[19]. The *Trpv1* cDNA was driven by the HSV thymidine kinase promoter (*TKp-Trpv1*) and the human *GLRA1* cDNA was driven by the HCMV promoter (*HCMVp-GLRA1*). We created two additional vectors for the capsaicin selection experiments. First, vTT was further modified to coexpress *DsRed2* gene–encoded RFP by recombining *HCMVp-RFP* cassette into the *UL41* locus to create vector vTTHR and a vector, vHP that encodes Trpv1 subunits lacking the channel pore-forming domain. The construction of the poreless Trpv1 plasmid is described in Supplementary Methods online.

Virus growth assays

We carried out infections for Trpv1 and GlyRα1 functional studies in suspension in 15-ml conical tubes (Falcon) containing DMEM with 10% FBS for Trpv1 studies and glycine-free MEM with glycine-depleted 10% dialyzed FBS for GlyRαl studies. Infections were rocked on a nutator platform for 1 h at 37 °C. The 250,000 cells/well, plated in 24-well plates containing required final concentrations of reagents in 1 ml of suitable media depending on the vector being used, and incubated at 37 °C. We collected supernatant samples at 24, 48 and 72 h.p.i. and titered them by standard viral plaquing assays[23]. We counted the number of plaques for each viral dilution and expressed them as viral p.f.u./ml of viral suspension. All viral titer measurements are reported from different supernatants collected from four independent experiments (n = 4).

Additional methods

Detailed descriptions of methods used for Ca^{+2} influx assays, MPT analysis, Southern blotting, immunostaining, patch clamp recordings and the primer sequences for poreless Trpv1 construction are available in Supplementary Methods.

Supplementary Material

Refer to Web version on PubMed Central for supplementary material.

Acknowledgments

We thank D. Fink for useful discussions and D. Julius for providing Trpv1 cDNA. Human GLRA1 cDNA was obtained from M.C. NDT9515223 was a gift from Neurogen Corp. Supported by grants from the US National Institutes of Health (NIH) National Institute of Diabetes and Digestive and Kidney Diseases 2P01 DK04493512A1 (J.C.G.); P01 DK044935-11 (J.C.G.); NIH National Cancer Institute 1R01 CA119298-01 (J.C.G.); NIH National Institute of Neurological Disorders and Stroke 5R01 NS44323-04 (J.C.G.); NIH National Institute of Arthritis and Musculoskeletal and Skin Diseases 5U54 AR050733-02 (J.C.G.); NIH National Heart, Lung and Blood Institute 2U01 HL066949-06 (J.C.G.), NIH R01 DK49430 (W.C.D.) and NIH R01 DK54171 (P.A.F.).

References

1. Hubner CA, Jentsch TJ. Ion channel diseases. Hum Mol Genet. 2002; 11:2435–2445. [PubMed: 12351579]
2. Kalso E. Sodium channel blockers in neuropathic pain. Curr Pharm Des. 2005; 11:3005–3011. [PubMed: 16178759]

3. Reis J, et al. Levetiracetam influences human motor cortex excitability mainly by modulation of ion channel function–a TMS study. Epilepsy Res. 2004; 62:41–51. [PubMed: 15519131]
4. Cheng JH, Kamiya K, Kodama I. Carvedilol and vesnarinone: new antiarrhythmic approach in heart failure therapy. Acta Pharmacol Sin. 2001; 22:193–200. [PubMed: 11742564]
5. Dutcher JP, et al. Phase II study of carboxyamidotriazole in patients with advanced renal cell carcinoma refractory to immunotherapy. Cancer. 2005; 104:2392–2399. [PubMed: 16222691]
6. Ye JH, Ponnudurai R, Schaefer R. Ondansetron: a selective 5-HT(3) receptor antagonist and its applications in CNS-related disorders. CNS Drug Rev. 2001; 7:199–213. [PubMed: 11474424]
7. Gao ZG, Jacobson KA. Keynote review: allosterism in membrane receptors. Drug Discov Today. 2006; 11:191–202. [PubMed: 16580596]
8. Bates IR, Wiseman PW, Hanrahan JW. Investigating membrane protein dynamics in living cells. Biochem Cell Biol. 2006; 84:825–831. [PubMed: 17215870]
9. Sullivan E, Tucker EM, Dale IL. Measurement of [Ca2+] using the fluorometric imaging plate reader (FLIPR). Methods Mol Biol. 1999; 114:125–133. [PubMed: 10081013]
10. Loukin SH, et al. Random mutagenesis reveals a region important for gating of the yeast K+ channel Ykc1. EMBO J. 1997; 16:4817–4825. [PubMed: 9305624]
11. Marconi P, et al. Replication-defective herpes simplex virus vectors for gene transfer in vivo. Proc Natl Acad Sci USA. 1996; 93:11319–11320. [PubMed: 8876133]
12. Gunthorpe MJ, et al. Identification and characterisation of SB-366791, a potent and selective vanilloid receptor (VR1/TRPV1) antagonist. Neuropharmacology. 2004; 46:133–149. [PubMed: 14654105]
13. Valenzano KJ, et al. N-(4-tertiarybutylphenyl)-4-(3-chloropyridin-2-yl) tetrahydropyrazine-1(2H)-carbox-amide (BCTC), a novel, orally effective vanilloid receptor 1 antagonist with analgesic properties: I. *in vitro* characterization and pharmacokinetic properties. J Pharmacol Exp Ther. 2003; 306:377–386. [PubMed: 12721338]
14. Gunthorpe MJ, Harries MH, Prinjha RK, Davis JB, Randall A. Voltage- and time-dependent properties of the recombinant rat vanilloid receptor (rVR1). J Physiol (Lond). 2000; 525:747–759. [PubMed: 10856126]
15. Sculptoreanu A, de Groat WC, Buffington CA, Birder LA. Protein kinase C contributes to abnormal capsaicin responses in DRG neurons from cats with feline interstitial cystitis. Neurosci Lett. 2005; 381:42–46. [PubMed: 15882787]
16. Sculptoreanu A, de Groat WC, Buffington CA, Birder LA. Abnormal excitability in capsaicin-responsive DRG neurons from cats with feline interstitial cystitis. Exp Neurol. 2005; 193:437–443. [PubMed: 15869946]
17. Copp J, Wiley S, Ward MW, van der Geer P. Hypertonic shock inhibits growth factor receptor signaling, induces caspase-3 activation, and causes reversible fragmentation of the mitochondrial network. Am J Physiol Cell Physiol. 2005; 288:C403–C415. [PubMed: 15456696]
18. Sontheimer H, et al. Functional chloride channels by mammalian cell expression of rat glycine receptor subunit. Neuron. 1989; 2:1491–1497. [PubMed: 2483325]
19. Cascio M, Schoppa NE, Grodzicki RL, Sigworth FJ, Fox RO. Functional expression and purification of a homomeric human alpha 1 glycine receptor in baculovirus-infected insect cells. J Biol Chem. 1993; 268:22135–22142. [PubMed: 8408073]
20. Garcia-Sanz N, et al. Identification of a tetramerization domain in the C terminus of the vanilloid receptor. J Neurosci. 2004; 24:5307–5314. [PubMed: 15190102]
21. Stavrovskaya IG, Kristal BS. The powerhouse takes control of the cell: is the mitochondrial permeability transition a viable therapeutic target against neuronal dysfunction and death? Free Radic Biol Med. 2005; 38:687–697. [PubMed: 15721979]
22. Srinivasan R, Glorioso JC. Novel modulators of the capsaicin receptor. Cellscience. 2007; 3:141–160.
23. Goins WF, Krisky DM, Wolfe DP, Fink DJ, Glorioso JC. Development of replication-defective herpes simplex virus vectors. Methods Mol Med. 2002; 69:481–507. [PubMed: 11987796]
24. Chen X, et al. Herpes simplex virus type 1 ICP0 protein does not accumulate in the nucleus of primary neurons in culture. J Virol. 2000; 74:10132–10141. [PubMed: 11024142]

25. Caterina MJ, et al. The capsaicin receptor: a heat-activated ion channel in the pain pathway. Nature. 1997; 389:783–784. [PubMed: 9349801]

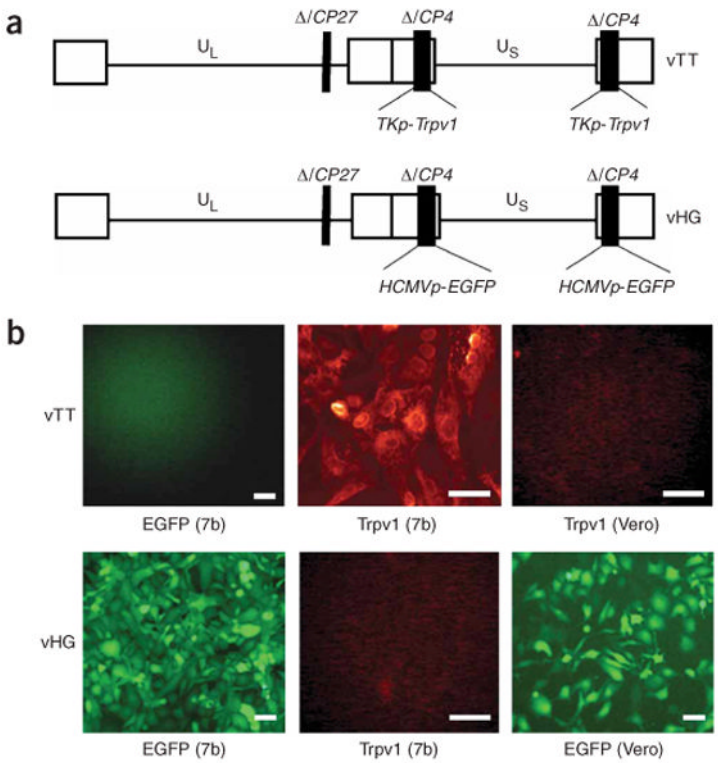

Figure 1.

HSV vector constructs and protein expression profiles. (**a**) vTT and vHG vectors contain deletions of the immediate early genes, *ICP4* and *ICP27*. In the genome of the vTT vector, a cassette coding for the rat Trpv1 receptor, driven by the *tk* early promoter (*TKp-Trpv1*) resides in the *ICP4* locus. In the genome of vHG, an HCMV immediate early promoter driving enhanced green fluorescent protein (*HCMVp*-EGFP) is inserted into both *ICP4* loci. (**b**) Protein expression profiles of vHG and vTT-infected complementing 7b and noncomplementing Vero cell lines are depicted. vTT-infected 7b cells do not express EGFP. *Trpv1* expression is under transcriptional control of an early HSV thymidine kinase promoter and is therefore limited to vTT-infected complementing 7b cells by immunostaining. EGFP is under transcriptional control of an immediate early HCMV promoter and is hence expressed by vector vHG in 7b as well as Vero cells. vHG-infected 7b cells do not express Trpv1 by immunostaining. Scale bars, 30 μm.

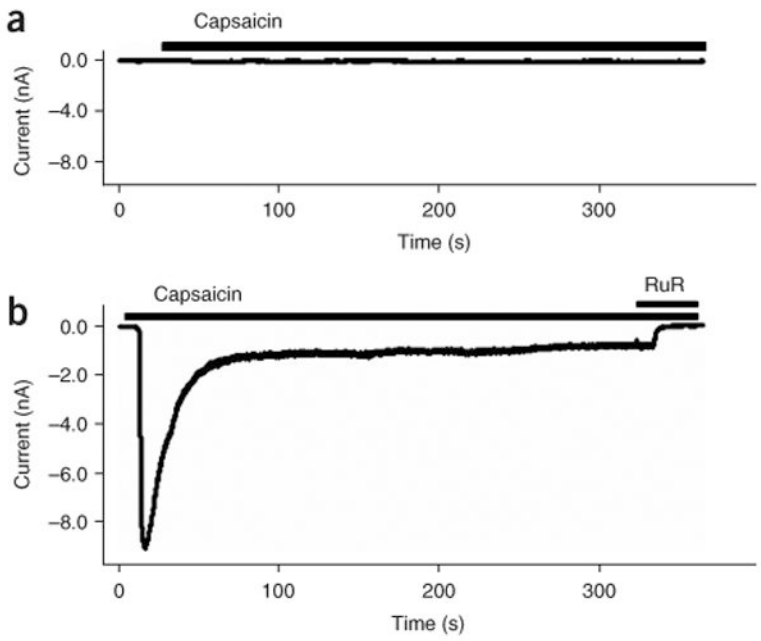

Figure 2.

Whole-cell patch-clamp recordings of vTT-expressed Trpv1 activation by capsaicin. (**a**) vHG-infected 7b cells do not respond to capsaicin stimulation. (**b**) vTT-infected 7b cells show a large biphasic inward current (8 nA) that desensitizes after stimulation with 0.5 μM capsaicin. Addition of ruthenium red (RuR; 5 μM) completely blocked the capsaicin current.

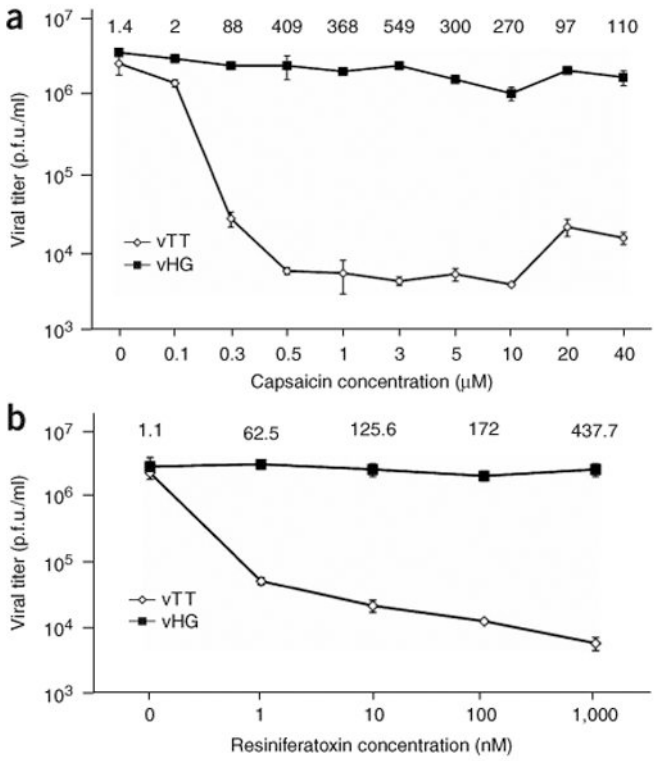

Figure 3.

Inhibition of vTT replication by Trpv1 agonists. (**a**) 7b-complementing cells were infected with vTT or vHG (control) virus and plated in culture medium containing increasing doses of capsaicin. Viral titers determined from supernatant medium at 72 h.p.i. are plotted against capsaicin concentration. Growth ratios, calculated as the ratio of vHG to vTT viral titers (p.f.u./ml) at each concentration of capsaicin are indicated at the top for each capsaicin concentration. Error bars, ± s.d., $n = 4$. (**b**) Complementing 7b cells infected with vTT or vHG (control) virus were plated in culture medium containing increasing doses of resiniferatoxin (0–1,000 nM final). Viral titers determined from supernatant samples are plotted against the resiniferatoxin concentration at 72 h post-infection. Growth ratios calculated as the ratio of vHG to vTT viral titers (p.f.u./ml) for each concentration of resiniferatoxin are indicated for each data point. Error bars, ± s.d.; $n = 4$.

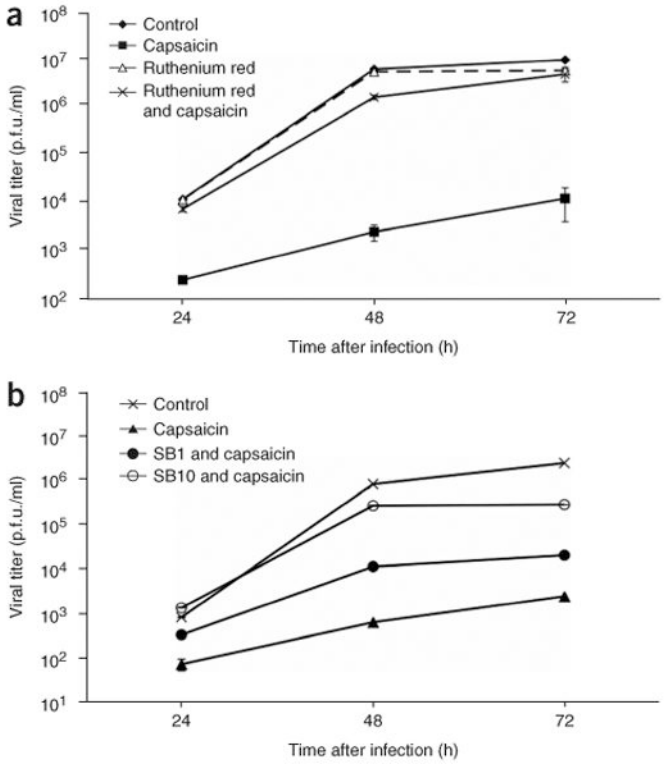

Figure 4.

Rescue of vTT replication by Trpv1 by known antagonists. (**a**) Viral titers from vTT-infected 7b cells (0.01 p.f.u./cell) are represented as growth curves at 24, 48 and 72 h.p.i., after separate incubation with either nothing (control), 3 μM capsaicin, 5 μM ruthenium red, or 5 μM ruthenium red and 3 μM capsaicin. Error bars, ± s.d.; $n = 4$. (**b**) Viral titers from vTT-infected 7b cells (0.01 p.f.u./cell) are represented as growth curves at 24, 48 and 72 h.p.i., after separate incubation with nothing (control), 3 μM capsaicin, 1 μM SB-366791 (SB1) and 0.5 μM capsaicin, and 10 μM SB-366791 (SB10) and 0.5 μM capsaicin. Error bars, ± s.d.; $n = 4$.

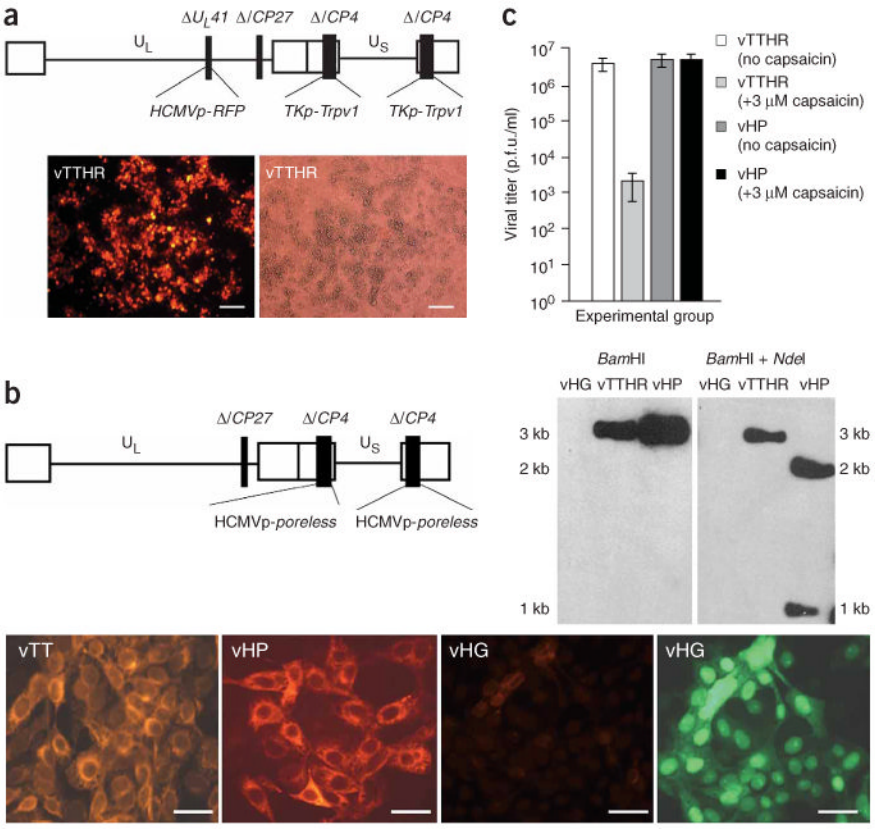

Figure 5.

Construction and characterization of vectors vTTHR and vHP. (**a**) vTTHR genomic structure (top), and fluorescence (bottom left) and brightfield (bottom right) images of vTTHR plaques in 7b cells. Scale bars, 100 μm. (**b**) vHP genomic structure (top left). A representative Southern blot probed with *Trpv1* cDNA (top right). The left two micrographs show immunostaining for Trvp1. The right two images were taken using red fluorescence or green fluorescence filters of the field of vHG infected 7b cells. Scale bars, 40 μm. (**c**) Effect of 3 μM capsaicin on vTTHR and vHP. Error bars, ± s.d.; $n = 4$.

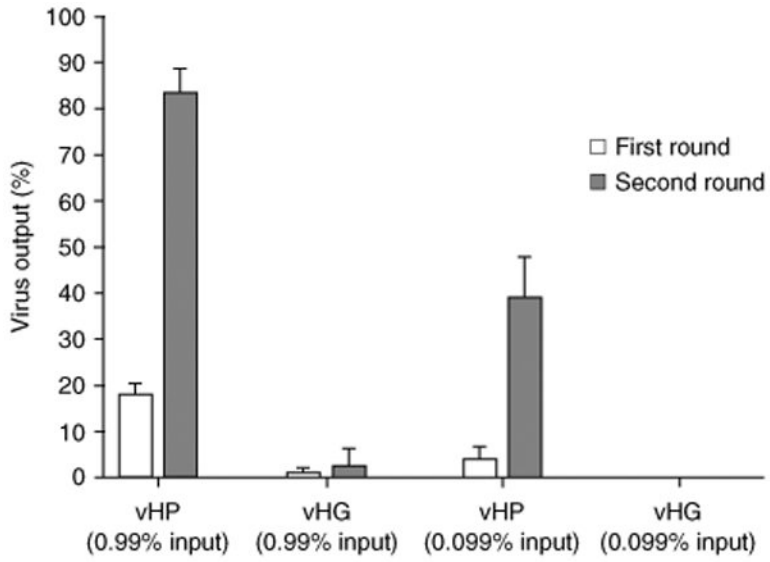

Figure 6.

Selection for vHP in coinfection experiments. Virus output after two rounds of selection with 3 μM capsaicin for coinfections of either vHP (percentage of total virus input was 0.99 or 0.099%) + vTTHR or vHG (percentage of total virus input was 0.99 or 0.099%) + vTTHR. Error bars, ± s.d.; $n = 4$.